Superconducting pairing symmetry and energy gaps of the two-orbital t–t'–J–J' model: comparisons with the ARPES experiments in iron pnictides

Superconducting pairing symmetry and energy gaps of the two-orbital t–t'–J–J' model: comparisons with the ARPES experiments in iron pnictides

Feng Lu[1,2] and Liang-Jian Zou[1,3]

[1] Key Laboratory of Materials Physics, Institute of Solid State Physics, Chinese Academy of Sciences, PO Box 1129, Hefei 230031, People's Republic of China
[2] Graduate School of the Chinese Academy of Sciences, Beijing 100049, People's Republic of China

E-mail: zou@theory.issp.ac.cn

Abstract
Motivated by the discovery of the iron-based superconductors, we present the theoretical results on the superconducting phase diagram, the temperature-dependent Fermi surface structures in normal state and the angle-resolved photoemission spectroscopy (ARPES) character of quasiparticles of the two-orbital t–t'–J–J' model. In the reasonable physical parameter region of $LaFeAsO_{1-x}F_x$, we find the superconducting phase is stable, and the pairing symmetry is weakly anisotropic and nodeless $d_{x^2-\eta y^2} + S_{x^2 y^2}$-wave, qualitatively in agreement with the ARPES experiments in iron pnictide superconductors. Nevertheless, the two ratios of the energy gaps to T_c deviate from the ARPES data, suggesting that a more elaborate theoretical model is needed.

(Some figures in this article are in colour only in the electronic version)

1. Introduction

Following the discovery of the first high-transition temperature superconductivity in copper-based compounds two decades ago [1], a second class of high-transition temperature superconductors has been recently reported in iron pnictides [2–6], in which the transition temperature T_c is as high as 56 K [7]. So far, intensive experimental [8–15] and theoretical [16–21] efforts have been devoted to understanding the nature of the new superconductors. Similar to cuprates, layered iron pnictides consist of conducting FeAs layers and ReO layers (Re represents rare earth elements, such as La, Ce, Pr, Nd, Sm, etc) which provide carriers for the FeAs layers. The ground state is an antiferromagnetic spin-density-wave (SDW) phase in undoped parent compounds LaOFeAs and $BaFe_2As_2$; the SDW order is suppressed by substituting a few per cent of O with F or Ba with K, and the new compounds enter the superconducting

(SC) phase below T_c. On the other hand, iron pnictides differ from cuprates in many aspects. Firstly, the undoped iron oxypnictides with the SDW order are poor but metallic conductors, rather than the *Néel* antiferromagnetic insulators in undoped cuprates; secondly, there exist well-defined and complicated Fermi surfaces (FS) in the normal state in $NdFeAsO_{1-x}F_x$ [22] and $Ba_{1-x}K_xFe_2As_2$ [23–25], significantly different from the situation in cuprates; and so on. These facts suggest that the ground states and the nature of SC of iron pnictides and cuprates are profoundly different.

To date, first-principles electronic structure calculations [16, 26–30] have shown that, in iron pnictides, Fe 3d orbits contribute the major spectral weight close to the Fermi energy; and the FS of LaFeAsO consists of two hole-type circles around the Γ point and two electron-type co-centered ellipses around the M point [31]. This implies that the multi-orbital character is dominant in the FeAs SC, in contrast to the single-orbital character in cuprates. Since the electron–phonon mediated pairing mechanism was precluded by Boeri *et al* [27],

the electronic and spin fluctuation mechanisms have been proposed as the driving force of the SC pairing [18, 19, 21, 32]. Presently, a few tight-binding multi-orbital models, such as the two-orbital models [33–35], the three-orbital ones [19] and the four-orbital ones [36], even the five-orbital models [17, 37], have been proposed to reproduce the FS character and the band structures near the Fermi level E_F in ReFeAsO$_{1-x}$F$_x$ and Ba$_{1-x}$K$_x$Fe$_2$As$_2$. Among these models, the two-orbital $t–t'–J–J'$ model [33, 34] is minimal and can reproduce the key characteristics of iron pnictides, such as the complicated FS topology, the multi-orbital degeneracy of the Fe 3d electrons [33, 34] and the band structures near E_F, as well as the stripe antiferromagnetic or SDW ground state [38].

In this newly discovered SC, the most intriguing issues are the pairing mechanism and pairing symmetry. To date, various possibilities of SC mechanism and pairing symmetry in iron-based SC have been proposed theoretically [18, 19, 21, 32, 33, 39–45] and experimentally [22, 24, 25, 46, 47]. Theoretically, the proposed SC pairing symmetries range from spin singlet d-wave [48, 49], s-wave [21, 32] or a mixture of S$_{x^2y^2}$-wave and d$_{x^2-y^2}$-wave [39] to spin triplet p-wave [18, 19]. Experimentally, the nature of the SC gap observed is also very different from author to author and from sample to sample, ranging from one gap [8] to two gaps [25, 46, 50], and from isotropic gap [24, 25] or anisotropic full gap [22] to line node [46]. Among these, the angle-resolved photoemission spectroscopy (ARPES) experiments [22, 24, 25], a kind of direct measurement of the quasiparticle spectra and the SC gaps, observed that the SC iron pnictides have two gaps. Both of the gaps are nodeless around their respective FS sheets. This is also different from the singly gapped cuprates. These disagreements among the experimental data and the theoretical results on the SC nature of iron pnictides show that more efforts are needed to unveil the mysterious nature of SC in iron pnictides.

To date, many experiments and theories have demonstrated that the electronic correlation in iron pnictides is strong, implying that iron pnictides are strongly correlated systems [51–56]. On the one hand, the ARPES experiment in Ba$_{0.6}$K$_{0.4}$Fe$_2$As$_2$ showed that the bandwidths near the Fermi surface display strong narrowing by a factor of 2 and strong mass renormalization by a factor of 4 [52], indicating a strong correlation effect; and the resonant excitations observed in the inelastic neutron scattering [51] and the anomalous electrical resistivity and thermopower in transport [54] are common evidence of strongly correlated superconductors. On the other hand, the dynamic mean-field theory has suggested that undoped iron pnictide is strongly correlated and close to the edge of a metal–insulator transition [55]; and the LDA + DMFT calculation based on the Monte Carlo solver by Anisimov *et al* [56] showed that the electron correlation plays an important role in the density of states near E_F and the band narrowing.

Then a question naturally arises as to why the parent iron pnictides display metallic behavior, rather than Mott insulators as in high-T_c cuprates. We attribute this to the multi-orbital character and the absence of the Jahn–Teller effect. In undoped cuprates, the Jahn–Teller distortion removes the degeneracy of the twofold e$_g$ orbit in copper and leads to an effective

single-orbital model. In contrast, the multibands involved in the formation of the Fermi surfaces in iron pnictides are almost degenerate, so the low-energy process in iron pnictide SC should be described by a multi-orbital model. When the Hund's coupling J_H is not large, the orbital fluctuation considerably suppresses the critical value of the intra-orbital Coulomb interaction, U_c, for the metal–insulator transition in the multi-orbital systems, in comparison with that in the single-orbital systems. For example, on the triangular lattice, the critical value $U_c = 12$ in the single-orbital system [57, 58], while, $U_c = 18.2$ in the two-orbital system [59]. Thus, for two systems in the strong correlation regime, the single-orbital system may be a Mott insulator, as seen in the parent phases of cuprates. However, the multi-orbital system may be a metal, as seen in the parent phases of iron pnictides.

To develop qualitative insight into the underlying physics, in this paper, we start with the minimal two-orbital $t–t'–J–J'$ model [34, 60], which has the same topology as the FS and the band structures of the iron-based SC, and obtain the mean-field phase diagram of the $t–t'–J–J'$ model, the quasiparticle spectra in normal state and SC phase, and the ARPES manifestation of the SC gaps. Our results demonstrate that the pairing symmetry d$_{x^2-\eta y^2}$ + S$_{x^2y^2}$ wave is stable in the reasonable parameter region for iron pnictides; two SC gaps qualitatively agree with the observations in ARPES experiments. However, a quantitative comparison between theory and experiment shows a more elaborate theoretical model is needed. The rest of this paper is organized as follows: we describe the $t–t'–J–J'$ model Hamiltonian and the self-consistent mean-field solution in section 2 and present the theoretical results on the SC phase diagram, the temperature evolution of the FS and SC gaps, and the ARPES spectra of the quasiparticle in sections 3 and 4 is devoted to the summary.

2. Model Hamiltonian and formulae

We describe the low-energy processes in iron pnictides with the two-orbital $t–t'–J–J'$ model:

$$H = H_{t-t'} + H_{J-J'}, \tag{1}$$

on a quasi-two-dimensional square lattice. This Hamiltonian consists of the tight-binding kinetic energy $H_{t-t'}$ and the interaction part $H_{J-J'}$. The kinetic energy term is

$$H_{t-t'} = \sum_{k\sigma} [(\varepsilon_{kxz} - \mu)c_{k1\sigma}^\dagger c_{k1\sigma} + (\varepsilon_{kyz} - \mu)c_{k2\sigma}^\dagger c_{k2\sigma} + \varepsilon_{kxy}(c_{k1\sigma}^\dagger c_{k2\sigma} + c_{k2\sigma}^\dagger c_{k1\sigma})]$$

with the notations

$$\varepsilon_{kxz} = -2t_1 \cos k_x - 2t_2 \cos k_y - 4t_3 \cos k_x \cos k_y,$$

$$\varepsilon_{kyz} = -2t_2 \cos k_x - 2t_1 \cos k_y - 4t_3 \cos k_x \cos k_y,$$

$$\varepsilon_{kxy} = -4t_4 \sin k_x \sin k_y,$$

where $c_{i\alpha\sigma}^\dagger$ creates a d$_{xz}$ ($\alpha = 1$) or d$_{yz}$ ($\alpha = 2$) electron with orbit α and spin σ at site R_i. The intra-orbital components of the nearest-neighbor (NN) hopping integrals $t_{ij}^{\alpha\beta}$ are $t_x^{11} =$

$t_1 = -1$, and $t_x^{22} = t_2 = 1.3$. The components of the next-nearest-neighbor (NNN) hopping integrals, $t_{ij}'^{\alpha\beta}$, are $t_3 = t_4 = -0.85$ [34]. μ is the chemical potential. Throughout this paper, all the energies are measured in units of $|t_1|$. The carrier concentration is equal to 0.18, which is a typical doping concentration in the iron-based SC [61].

The interaction term contains an NN and an NNN antiferromagnetic spin coupling:

$$H_{J-J'} = J \sum_{\langle ij \rangle \alpha\beta} (\vec{S}_{i\alpha} \cdot \vec{S}_{j\beta} - \tfrac{1}{4} n_{i\alpha} \cdot n_{j\beta})$$
$$+ J' \sum_{\langle\langle ij \rangle\rangle \alpha\beta} (\vec{S}_{i\alpha} \cdot \vec{S}_{j\beta} - \tfrac{1}{4} n_{i\alpha} \cdot n_{j\beta}) \quad (2)$$

where J and J' are the NN and the NNN spin coupling strengths, respectively. $\vec{S}_{i\alpha}$ is the spin operator of the electron in the α orbit at R_i and $n_{i\alpha}$ is the particle number operator. The orbital indices α and β run over 1 and 2. Formally, the t–t'–J–J' model can be derived from the two-orbital Hubbard model in the atomic limit [60], which is believed to describe the SDW ground state in undoped iron-based oxypnictides [38, 62].

Notice that the d_{xz} and d_{yz} orbits are spatially anisotropic, in other words, the intra-orbital hopping integral along the x direction is inequivalent to that along the y direction for each orbit, as one can see from $|t_1| \neq |t_2|$. Due to the inequivalence of the different directions in different orbits, the amplitude of the SC gap of the local pairing along the x direction may be not equal to that along the y direction in each orbit. Thus, the single-orbital d-wave or s-wave SC order parameter, in which the SC gap has fourfold symmetry of rotational invariance in the xy plane, is not suitable for describing the pairing symmetry of the intra-orbital SC order parameters in this multi-orbital system. Considering all of the possible kinetic correlations and the SC pairings for the NN and NNN sites along different directions, we introduce the following order parameters:

$$P_{x/y}^{\alpha} = \langle c_{i\alpha\sigma}^{\dagger} c_{j\alpha\sigma} \rangle, \qquad (j = i \pm \hat{x}/\hat{y})$$
$$P_{xy}^{1/2} = \langle c_{i1\sigma}^{\dagger} c_{j2\sigma} \rangle, \qquad (j = i \pm \hat{x}/\hat{y})$$
$$P_3^{\alpha} = \langle c_{i\alpha\sigma}^{\dagger} c_{j\alpha\sigma} \rangle, \qquad (j = i \pm (\hat{x} \pm \hat{y}))$$
$$P_{xy}^{3/4} = \langle c_{i1\sigma}^{\dagger} c_{j2\sigma} \rangle, \qquad (j = i \pm (\hat{x} \pm \hat{y})) \quad (3)$$
$$\Delta_{x/y}^{1\alpha} = J \langle c_{i\alpha\uparrow}^{\dagger} c_{j\alpha\downarrow}^{\dagger} \rangle, \qquad (j = i \pm \hat{x}/\hat{y})$$
$$\Delta_{x\pm y}^{2\alpha} = J' \langle c_{i\alpha\uparrow}^{\dagger} c_{j\alpha\downarrow}^{\dagger} \rangle, \qquad (j = i \pm (\hat{x} \pm \hat{y})).$$

Here $P_{x/y}^{\alpha}$ and $P_{xy}^{1/2}$ (P_3^{α} and $P_{xy}^{3/4}$) are the kinetic average of the NN (NNN) intra-orbital and inter-orbital hopping integrals. These terms are neglected in Seo *et al*'s mean-field ansatz [39]. $\Delta_{x/y}^{1\alpha}$ ($\Delta_{x\pm y}^{2\alpha}$) is the mean-field amplitude of the local NN (NNN) pairing order parameter in the α orbit. The inter-orbital pairing parameter $\langle c_{i1\uparrow}^{\dagger} c_{j2\downarrow}^{\dagger} \rangle$ is very small and hence is neglected [39].

With these parameters, one can decouple the interaction terms in equation (2) within the framework of the self-consistent mean-field approximation and obtain the mean-field Hamiltonian, $H_{\rm MF} = \sum_k \Psi(k)^{\dagger} A(k) \Psi(k) + {\rm const}$. Here

$$\Psi(k) = (c_{k,1,\uparrow}, c_{-k,1,\downarrow}^{\dagger}, c_{k,2,\uparrow}, c_{-k,2,\downarrow}^{\dagger}):$$

$$A(k) = \begin{pmatrix} \epsilon_{k1\uparrow} - \mu & \Delta_1^*(k) & \epsilon_{k12} & 0 \\ \Delta_1(k) & -\epsilon_{k1\downarrow} + \mu & 0 & -\epsilon_{k12} \\ \epsilon_{k12} & 0 & \epsilon_{k2\uparrow} - \mu & \Delta_2^*(k) \\ 0 & -\epsilon_{k12} & \Delta_2(k) & -\epsilon_{k2\downarrow} + \mu \end{pmatrix}, \quad (4)$$

and const is the collection of all the constant energy terms from the mean-field decoupling. The modified intra-orbital and inter-orbital kinetic energy is

$$\varepsilon_{k1\sigma} = \varepsilon_{kxz} - 2J(P_x^1 \cos k_x + P_y^1 \cos k_y)$$
$$- 4J' P_3^1 \cos k_x \cos k_y - 4(J + J')(\langle n_{1\sigma} \rangle + \langle n_{2\sigma} \rangle)$$
$$\varepsilon_{k2\sigma} = \varepsilon_{kyz} - 2J(P_x^2 \cos k_x + P_y^2 \cos k_y)$$
$$- 4J' P_3^2 \cos k_x \cos k_y - 4(J + J')(\langle n_{1\sigma} \rangle + \langle n_{2\sigma} \rangle)$$
$$\varepsilon_{k12} = \varepsilon_{kxy} - 2J(P_{xy}^1 \cos k_x + P_{xy}^2 \cos k_y)$$
$$- 4J'(P_{xy}^3 \cos(k_x + k_y) + P_{xy}^4 \cos(k_x - k_y)). \quad (5)$$

The SC order parameter $\Delta_{\alpha}(k)$ of each orbital channel in the momentum space is

$$\Delta_{\alpha}(k) = -4(\Delta_x^{1\alpha} \cos k_x + \Delta_y^{1\alpha} \cos k_y)$$
$$- 4(\Delta_{x+y}^{2\alpha} \cos(k_x + k_y) + \Delta_{x-y}^{2\alpha} \cos(k_x - k_y))$$
$$= -4\Delta_x^{1\alpha}[(\cos(k_x) \pm \eta_{1\alpha} \cos(k_y))$$
$$+ \xi_{\alpha}(\cos(k_x + k_y) \pm \eta_{2\alpha} \cos(k_x - k_y))]. \quad (6)$$

Thus the SC pairing symmetry of the α orbit is determined by $(\cos(k_x) \pm \eta_{1\alpha} \cos(k_y)) + \xi_{\alpha}(\cos(k_x + k_y) \pm \eta_{2\alpha} \cos(k_x - k_y))$. Where $\xi_{\alpha} = \Delta_{x+y}^{2\alpha}/\Delta_x^{1\alpha}$, the anisotropic factors, $\eta_{1\alpha} = |\Delta_y^{1\alpha}/\Delta_x^{1\alpha}|$ and $\eta_{2\alpha} = |\Delta_{x-y}^{2\alpha}/\Delta_{x+y}^{2\alpha}|$, are positive. $\pm$ denotes the relative phase of $\Delta_x^{1\alpha}$ with respect to $\Delta_y^{1\alpha}$ or $\Delta_{x-y}^{2\alpha}$ to $\Delta_{x+y}^{2\alpha}$.

To characterize the complicated SC order parameters in different parameter regions, we define the $S_{x^2+\eta y^2}$ wave or $d_{x^2-\eta y^2}$ wave as the SC symmetry when $\Delta_{\alpha} \propto \cos(k_x) + \eta \cos(k_y)$ or $\Delta_{\alpha} \propto \cos(k_x) - \eta \cos(k_y)$. It reduces to the conventional $S_{x^2+y^2}$ wave or $d_{x^2-y^2}$ wave SC symmetry at $\eta = 1$. We also define the $S_{\eta x^2 y^2}$ wave or d_{xy} wave as the SC symmetry when $\Delta_{\alpha} \propto \cos(k_x + k_y) + \eta \cos(k_x - k_y)$ or $\Delta_{\alpha} \propto \cos(k_x + k_y) - \eta \cos(k_x - k_y)$. It reduces to the familiar $S_{x^2 y^2}$-wave or d_{xy}-wave SC symmetry at $\eta = 1$.

Diagonalizing the matrix $A(k)$ by an unitary transformation $U(k)$, $U(k)^{\dagger} A(k) U(k)$, and minimizing the free energy of the system with respect to these parameters in equation (3), one obtains the self-consistent equations:

$$n_{(1/2)\uparrow} = \frac{1}{N} \sum_{k,\alpha} U_{(1/3)\alpha}^*(k) U_{(1/3)\alpha}(k) f(E_{\alpha}(k))$$

$$n_{(1/2)\downarrow} = \frac{1}{N} \sum_{k,\alpha} U_{(2/4)\alpha}^*(k) U_{(2/4)\alpha}(k)(1 - f(E_{\alpha}(k)))$$

$$P_{x/y}^{1/2} = \frac{1}{N} \sum_{k,\alpha} \cos k_{x/y} U_{(1/3)\alpha}^*(k) U_{(1/3)\alpha}(k) f(E_{\alpha}(k))$$

$$P_3^{1/2} = \frac{1}{N} \sum_{k,\alpha} \cos k_x \cos k_y U_{(1/3)\alpha}^*(k) U_{(1/3)\alpha}(k) f(E_{\alpha}(k))$$

$$P_{xy}^{1/2} = \frac{1}{N} \sum_{k,\alpha} \cos k_{x/y} U_{1\alpha}^*(k) U_{3\alpha}(k) f(E_{\alpha}(k))$$

$$P_{xy}^{3/4} = \frac{1}{N} \sum_{k,\alpha} \cos(k_x \pm k_y) U_{1\alpha}^*(k) U_{3\alpha}(k) f(E_\alpha(k))$$

$$\Delta_{x/y}^{1(1/2)} = \frac{J}{N} \sum_{k,\alpha} \cos k_{x/y} U_{(1/3)\alpha}^*(k) U_{(2/4)\alpha}(k) f(E_\alpha(k))$$

$$\Delta_{x\pm y}^{2(1/2)} = \frac{J'}{N} \sum_{k,\alpha} \cos(k_x \pm k_y) U_{(1/3)\alpha}^*(k) U_{(2/4)\alpha}(k) f(E_\alpha(k))$$

$$(7)$$

where $E_\alpha(k)$ is the Bogoliubov quasiparticle eigenvalues obtained from H_{MF}, and $f(E)$ is the Fermi–Dirac distribution function, $f(E) = 1/(1 + \exp(E/k_B T))$. $U_{\alpha\beta}(k)$ denotes the (α, β) element of the 4×4 unitary matrix $U(k)$.

With these self-consistent equations, we could obtain not only the ground state phase diagram, but also the temperature dependence of the FS in the normal state and the quasiparticle spectra in the normal and SC states. In fact, the intra-orbital hopping integral of the d_{yz} orbit is symmetric with that of the d_{yz} orbit under a coordinate transformation $(x, y, z) \leftarrow (y, x, z)$. Due to this symmetry, the SC order parameters $\Delta_2(k)$ can be obtained from $\Delta_1(k)$ under the coordinate transformation. Therefore, we mainly focus the properties of the SC order parameters $\Delta_1(k)$ in the first orbit d_{xz}. Nevertheless, the global SC pairing order parameter of the two-orbital t–t'–J–J' model should be rotationally symmetric in the xy plane, as we can see from the Hamiltonian equation (1), and later in figure 3.

3. Theoretical results and discussions

In this section, we first present the phase diagram of the t–t'–J–J' model and discuss the SC pairing symmetry. Then we compare the theoretical results with the ARPES experimental observations.

The J'–J phase diagram of the t–t'–J–J' model at carrier concentration $x = 0.18$ is shown in figure 1(a). Different from Seo *et al*'s phase diagram [39], we obtain five stable phases in the present model. The first one is a normal phase in the small J and J' region, denoted by N in figure 1(a). Obviously, when the superexchange coupling J and J' are too small to provide the SC pairing glue, the kinetic energy is dominant, and the electrons stay in the normal state, which is analogous to the single-orbital t–J model [63]. Among the four SC phases mediated through the spin fluctuations, a large NN spin coupling J and a small NNN spin coupling J', or $J \gg J'$, favor the $S_{x^2+\eta y^2}$ (here and below $\eta_1 = \eta$) SC phase with the gap $\Delta_1(k) \propto \cos(k_x) + \eta \cos(k_y)$, where the pairing symmetry is the combination of the $S_{x^2+y^2}$-wave and the $d_{x^2-y^2}$-wave components, as seen in the shadowed region with no line in figure 1(a). The $S_{x^2+\eta y^2}$ symmetry arises from the major contribution of the NN spin coupling J term. The NNN spin coupling contributes very little to $\Delta_1(k)$ due to $J \gg J'$.

On the other hand, small NN spin coupling J and large NNN spin coupling J' favor the $S_{x^2 y^2}$ SC phase with the symmetry $\Delta_1(k) \propto \cos(k_x + k_y) + \cos(k_x - k_y)$, as seen in the shadowed region with the vertical line in figure 1(a), which is mainly attributed to the NNN spin coupling. In this
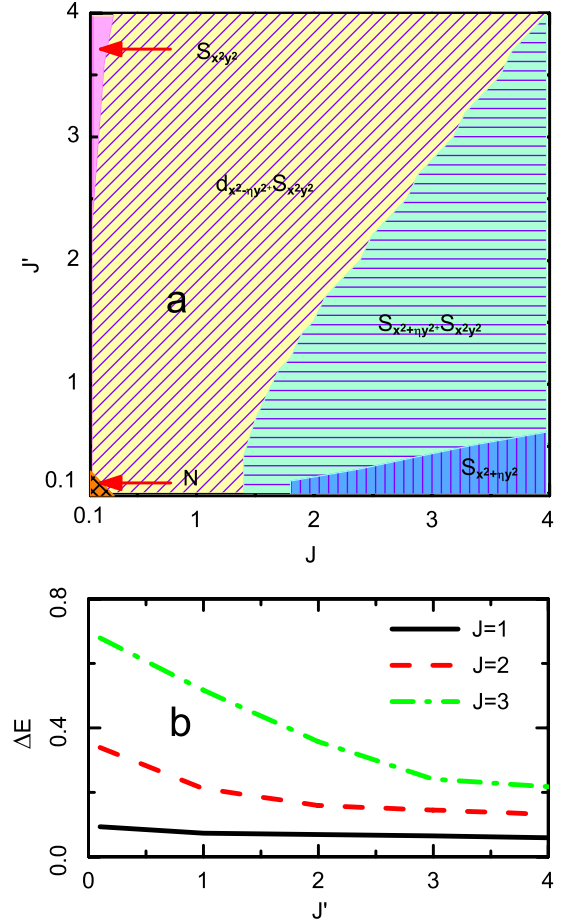

Figure 1. (a) SC phase diagram of the t–t'–J–J' model for the d_{xz} orbit at the carrier concentration $x = 0.18$. N denotes the normal state, the other four phases are SC with different pairing symmetries. (b) The energy difference ΔE between Seo *et al*'s [39] and our ground states versus the NNN spin coupling J' at different J, $J = 1$, 2 and 3, respectively.

situation, $\Delta_1(k)$ is almost isotropic in the xy plane due to the isotropy of the dominant NNN hopping integrals in the xy plane. The SC order parameter becomes complicated when J and J' compete with each other. As seen in figure 1(a), the pairing symmetry of the SC phase in the shadowed region with the transverse line of figure 1(a) is the combination of the $S_{x^2+\eta y^2}$ and the $S_{x^2 y^2}$ components, and the symmetry of the SC phase in the shadowed region with the slash of figure 1(a) is the combination of the $d_{x^2-\eta y^2}$ and the $S_{x^2 y^2}$ components.

It is interesting to ask in which region the realistic parameters of the iron pnictides fall. From the first-principles calculations, Ma *et al* suggested that $J \approx J' \approx 0.05 \text{ eV}/S^2$ [62], where S is the spin of each Fe ion. When the hopping integral $|t_1| \approx 0.1$–0.5 eV, such a set of parameters falls in the yellow region in figure 1(a), implying that the FeAs SC should have the $d_{x^2-\eta y^2} + S_{x^2 y^2}$ SC symmetry and the anisotropic factor η is not equal to 1. Also, some other authors suggested other parameters for the FeAs SC, for example, Seo *et al* [39] proposed that $J = 0.25$ and $J' = 0.5$; and Si *et al* [38] thought that $J > J'/2$. This shows that further effort is needed to obtain more accurate interaction parameters in iron pnictides.
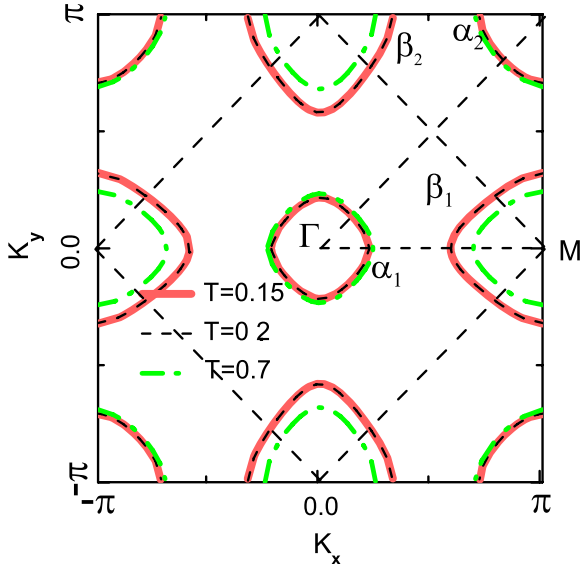
Figure 2. The Fermi surface topology in the large Brillouin zone at different temperatures: $T = 0.15$ (solid line), 0.2 (dashed line) and 0.7 (dot-dashed line). Dashed square outlines the reduced Brillouin zone. The theoretical parameters: $J = 0.3$, $J' = 0.7$; the other parameters are the same as those in figure 1.

Figure 3. The angle dependence of the SC gaps near the small hole FS (α_1) and the large hole FS (α_2) around the Γ point in the polar coordinate system. The doping concentration $x = 0.18$. Theoretical parameters: case I, $J = 0.3$, $J' = 0.7$ (open squares and circles); and case II, $J = 0.7$, $J' = 0.3$ (solid squares and circles).

We notice that Seo *et al*'s J–J' parameters also fall in the yellow region in figure 1(a), i.e. the SC pairing symmetry is $d_{x^2-\eta y^2} + S_{x^2 y^2}$ type, rather than the $\delta_s S_{x^2 y^2} \pm \delta_d d_{x^2-y^2}$ SC type with $\eta = 1$ (here δ_s and δ_d are the weights of the $S_{x^2-y^2}$ wave and the $d_{x^2-y^2}$ wave component, respectively). In figure 1(b), we compare the ground state energy difference between theirs and ours, and find that the ground state energy in the present SC phase, E_η, is lower than the E_d in Seo *et al*'s paper [39]. Figure 1(b) shows the J' dependence of the ground state energy difference, $\Delta E = E_d - E_\eta$, between the two SC phases at different J. It is clearly that, over a wide J–J' range, the $d_{x^2-\eta y^2} + S_{x^2 y^2}$ phase is always more stable than the $\delta_s S_{x^2 y^2} \pm \delta_d d_{x^2-y^2}$ phase. Thus the $d_{x^2-\eta y^2} + S_{x^2 y^2}$ wave is most likely the SC pairing symmetry in iron pnictide SC.

To concretely discuss the properties of the SC state and the normal state, and compare the theory with the ARPES experimental results, in what follows we focus on two sets of typical superexchange coupling parameters, case I: $J = 0.3$ and $J' = 0.7$, i.e. the NN spin coupling is weaker than the NNN coupling; and case II: $J = 0.7$ and $J' = 0.3$, i.e. the NN spin coupling is stronger than the NNN coupling. In both of the situations, the parameters fall in the shadowed region with the slash in figure 1(a), so the SC pairing symmetries are the $d_{x^2-\eta y^2} + S_{x^2 y^2}$ wave. We present the temperature evolution of the FS in the normal state in figure 2 for case I with $J = 0.3$ and $J' = 0.7$. The FS topology for case II with $J = 0.7$ and $J' = 0.3$ is almost identical to figure 2, and hence is not plotted. From figure 2, one sees that, in the large Brillouin zone (BZ) associated with the present t–t'–J–J' model with one Fe atom per unit cell, there exist two hole-like FS sheets (α_1 and α_2) around the Γ point and two electron-like FS sheets (β_1 and β_2) around the M point. This is in agreement with the ARPES experiment [25] and consistent with the first-principles
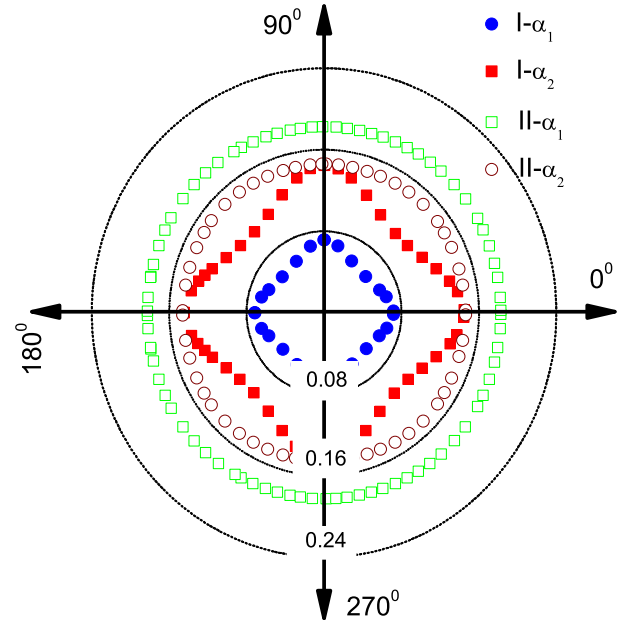
electronic structures calculations [16, 26–30]. Interestingly, the hole-like FS sheets expand a little with the increasing temperature; in contrast, the electron-like FS sheets shrink considerably. This indicates that the electron-like FS sheet may play a more important role in the low-energy processes in finite temperatures.

The ARPES experiment provides direct information about the quasiparticle spectra in the normal state and the pairing symmetry of the SC gaps in the SC state. In this paragraph, we present our theoretical results and compare them with experimental observation. Figure 3 shows the SC gap characteristics of the t–t'–J–J' model for the two sets of parameters in cases I and II. In both cases, two distinct gaps open on the hole-like FS sheets, α_1 and α_2, as seen in figure 2. The presence of two different SC gaps demonstrates the nature of a multi-gap SC in the t–t'–J–J' model. Our results show that, for case I, the SC gap structure exhibits a nearly isotropic symmetry with invisible anisotropy, as seen in figure 3. A large SC gap opens on the small hole FS sheet (α_1) and a small SC gap opens on the large hole FS sheet (α_2). For case II, the angular dependence of the SC gaps is visible, exhibiting weak spatial anisotropy. The oscillation amplitude is about 16%. However, the amplitudes of the SC gaps on the different FS, α_1 and α_2, are in contrast to these in case I, i.e. a small SC gap opens on the small FS sheet (α_1) and a large SC gap opens on the large hole FS sheet (α_2).

One finds that, in case I, the anisotropy of the SC gaps is very weak, consistent with Zhou *et al*'s [24] and Ding *et al*'s [25] ARPES data. In case II, the SC gaps with about 16% anisotropy are in agreement with the ARPES experiment by Kondo *et al* [22]. Note that, in case II, such spatial anisotropy is still under the resolution of the ARPES
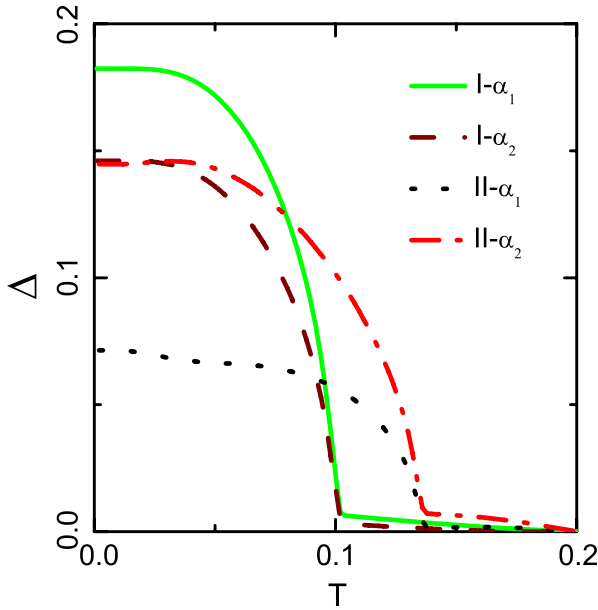
Figure 4. The temperature dependence of the SC gaps near the small hole FS (α_1) and the large hole FS (α_2) around the Γ point along the $\theta = 0°$ direction in the polar coordinate system. The theoretical parameters are the same as those in figure 3.

experiment and hence does not conflict with Zhou *et al*'s [24] and Ding *et al*'s [25] observation. It is the $d_{x^2-\eta y^2} + S_{x^2 y^2}$-wave pairing symmetry that leads to weakly anisotropy and nodeless SC gap structures, although the $d_{x^2-\eta y^2}$-wave pairing has nodes in the line $\cos k_x - \eta \cos k_y = 0$ and the $S_{x^2 y^2}$-wave pairing has nodes in the lines $k_x = \pm\pi/2$ or $k_y = \pi/2$. The mixed SC pairing symmetry, $d_{x^2-\eta y^2} + S_{x^2 y^2}$, diminishes the nodes, so the system exhibits weakly anisotropic and nodeless s-wave-like SC gaps on the FS sheets.

Figure 4 shows the temperature dependence of the SC energy gaps on the two hole-like FS sheets along the $\theta = 0°$ direction in the polar coordinate system for the two sets of parameters. With the increasing temperature, the two SC energy gaps decrease monotonically and vanish simultaneously, as observed in the ARPES experiments [24, 25]. Obviously, the SC–normal state transition is a second-order phase transition. For case I, the magnitude of the gap on the small FS (α_1) is larger than that on the large FS (α_2) in the Γ point, in agreement with the ARPES results [24, 25]. In contrast, for case II, the magnitude of the gap on the small FS (α_1) is smaller than that on the large FS (α_2) in the Γ point, which disagrees with the experiment [24, 25]. These indicate that the first set of parameters in case I is more suitable for describing the FeAs SC.

From the present theoretical results in figure 4, we find that, in case I, the ratios of the SC energy gaps to the transition temperature are $2\Delta_1/k_B T_c = 3.6$ for the large gap and $2\Delta_2/k_B T_c = 2.9$ for the small gap, respectively. The ratio of the large SC gap around the small FS sheet to the small one around the large FS sheet gives rise to $\Delta_1/\Delta_2 = 1.25$. These theoretical results significantly deviate from the ARPES experimental data [25]. In case II, $\Delta_1/\Delta_2 = 2$, in agreement

with [23]: however, the ratios of these two gaps with respect to T_c, $2\Delta_\alpha/k_B T_c$, also strongly disagree with [23]. These facts demonstrate that there exist some essential shortages in the present $t–t'–J–J'$ model or in the self-consistent field method. One also notices that, for case II, the decline of the two SC gaps with increasing temperature is not smooth, which comes from the fact that the different local pairing order parameters, $\Delta_{x/y}^{1\alpha}$ and $\Delta_{x\pm y}^{2\alpha}$, interplay with each other, reflecting the anisotropic pairing symmetry in case II.

From the preceding discussions, we find that many unusual properties in the normal state and the SC phase of newly discovered FeAs SC could be qualitatively interpreted in the two-orbital $t–t'–J–J'$ model, showing that, to some extent, this model is a good approximation to describe the iron pnictide SC. Within this scenario, the mixing pairing symmetry with the $d_{x^2-\eta y^2} + S_{x^2 y^2}$ wave contributes to the weakly anisotropic and nodeless SC gaps. Such a pairing symmetry assembles the characteristics of the usual d-wave and s-wave, and hence shares the properties of the usual d-wave SC, like cuprates, and the s-wave SC, such as MgB$_2$ [24]. Nevertheless, to quantitatively compare the theoretical results with the experimental observation, more subtle band structures of the $t–t'–J–J'$ model are expected.

We notice that Chubukov *et al* [64] suggested another possibility for the pairing symmetry of the iron pnictide SC. They found that, in the itinerant and weak-interacting multi-orbital model, the extended s-wave symmetry is stable in the SC ground state, similar to the $S_{x^2 y^2}$ pairing state in the sufficiently large J' parametric region in our phase diagram. Such a resemblance is not surprising since the fermiology and the fluctuation wavevector in the reciprocal space, i.e. the magnetic excitations in our scenario and the orbital excitations in Chubukov *et al*'s, predetermine the same pairing symmetry, as pointed out by Mazina *et al* [65]. However, one should keep in mind that our pairing mechanism is different for theirs. In their scenario, the pairing mechanism is mediated through the intra-band pairing hopping term, not necessarily due to spin fluctuations in our theory. So, there is a great difference between their theory and ours.

Also, one should keep in mind that a completely quantitative comparison between the theory and experiment is still difficult, since the present two-orbital $t–t'–J–J'$ model only describes the topology structure of the FS of the FeAs SC, and does not contain all the details of the FS and the band structures in iron pnictide compounds. On the other hand, in the realistic material, the spin couplings, J and J', might be the strong asymmetry [66, 67], which is not taken into account in the present $t–t'–J–J'$ model. Hence, we expect that the more elaborate tight-binding parameters and anisotropic coupling $J–J'$ model will improve the present results in a future study. Also the present constrained mean-field approximation needs to be further improved.

4. Summary

In summary, starting with the two-orbital $t–t'–J–J'$ model, we obtain the mean-field superconducting phase diagram at the carrier concentration $x = 0.18$ and find four stable

superconducting phases with different pairing symmetries. For the possible $LaO_{1-x}F_xFeAs$ parameters, a nodeless and weakly anisotropic $d_{x^2-\eta y^2} + S_{x^2 y^2}$-wave gap structure emerges. Due to the multi-orbital character, the ratio of the gaps open on the small hole Fermi surfaces to that on the large hole Fermi surfaces disagrees with the angle-resolved photoemission spectra data. A more elaborate theoretical model is expected for describing the nature of FeAs superconductors.

Acknowledgments

References

[1] Bednorz J G and Muller K A 1986 *Z. Phys.* B **64** 189
[2] Kamihara Y, Watanabe T, Hirano M and Hosono H 2008 *J. Am. Chem. Soc.* **130** 3296
[3] Chen G F *et al* 2008 *Phys. Rev. Lett.* **101** 057007
Chen G F *et al* 2008 *Phys. Rev. Lett.* **100** 247002
[4] Chen X H *et al* 2008 *Nature* **453** 761
[5] Ren Z-A *et al* 2008 *Mater. Res. Innovat.* **12** 105
[6] Wen H-H *et al* 2008 *Europhys. Lett.* **82** 17009
[7] Wu G *et al* 2009 *J. Phys.: Condens. Matter* **21** 142203
[8] Chen T Y *et al* 2008 *Nature* **453** 1224
[9] de la Cruz C *et al* 2008 *Nature* **453** 899
[10] Hunte F *et al* 2008 *Nature* **453** 903
[11] Jia X *et al* 2008 *Chin. Phys. Lett.* **25** 3765 arXiv:0806.0291
[12] Liu H *et al* 2008 *Chin. Phys. Lett.* **25** 3761
[13] Liu C *et al* 2008 arXiv:0806.2147
Liu C *et al* 2008 *Phys. Rev. Lett.* **101** 177005
[14] Hashimoto K *et al* 2009 *Phys. Rev. Lett.* **102** 017002
[15] Liu H *et al* 2008 *Phys. Rev.* B **78** 184514
[16] Mazin I I, Singh D J, Johannes M D and Du M H 2008 *Phys. Rev. Lett.* **101** 057003
[17] Kuroki K *et al* 2008 *Phys. Rev. Lett.* **101** 087004
[18] Dai X, Fang Z, Zhou Y and Zhang F C 2008 *Phys. Rev. Lett.* **101** 057008
[19] Lee P A and Wen X G 2008 arXiv:0804.1739
[20] Yao Z J, Li J X and Wang Z D 2009 *New J. Phys.* **11** 025009
[21] Wang F *et al* 2009 *Phys. Rev. Lett.* **102** 047005
[22] Kondo T *et al* 2008 *Phys. Rev. Lett.* **101** 147003
[23] Wray L *et al* 2008 *Phys. Rev.* B **78** 184508
[24] Zhao L *et al* 2008 *Chin. Phys. Lett.* **25** 4402
[25] Ding H *et al* 2008 *Europys. Lett.* **83** 47001
[26] Singh D and Du M-H 2008 *Phys. Rev. Lett.* **100** 237003
[27] Boeri L, Dolgov O V and Golubov A A 2008 *Phys. Rev. Lett.* **101** 026403
[28] Cao C, Hirschfeld P J and Cheng H-P 2008 *Phys. Rev.* B **77** 220506
[29] Ma F and Lu Z-Y 2008 *Phys. Rev.* B **78** 033111
[30] Lebègue S 2007 *Phys. Rev.* B **75** 035110
[31] Zhang H-J, Xu G, Dai X and Fang Z 2009 *Chin. Phys. Lett.* **26** 017401
[32] Nomura T *et al* 2008 *Supercond. Sci. Technol.* **21** 125028
[33] Han Q, Chen Y and Wang Z D 2008 *Europhys. Lett.* **82** 37007
[34] Raghu S *et al* 2008 *Phys. Rev.* B **77** 220503(R)
[35] Baskaran G 2008 arXiv:0804.1341
[36] Korshunov M M and Eremin I 2008 *Phys. Rev.* B **78** 140509(R)
[37] Haule K, Shim J H and Kotliar G 2008 *Phys. Rev. Lett.* **100** 226402
[38] Si Q and Abrahams E 2008 *Phys. Rev. Lett.* **101** 076401
[39] Seo K, Bernevig B A and Hu J P 2008 *Phys. Rev. Lett.* **101** 206404
[40] Daghofer M *et al* 2008 *Phys. Rev. Lett.* **101** 237004
[41] Graser S *et al* 2009 *New J. Phys.* **11** 025016
[42] Parish M M, Hu J P and Bernevig B A 2008 *Phys. Rev.* B **78** 144514
[43] Yanagi Y, Yamakawa Y and Ono Y 2008 *J. Phys. Soc. Japan* **77** 123701
[44] Ikeda H 2008 *J. Phys. Soc. Japan* **77** 123707
[45] Vorontsov A B, Vavilov M G and Chubukov A V 2009 *Phys. Rev.* B **79** 060508
[46] Matano K *et al* 2008 *Europhys. Lett.* **83** 57001
[47] Ahilan K *et al* 2008 *Phys. Rev.* B **78** 100501(R)
[48] Mu G *et al* 2008 *Chin. Phys. Lett.* **25** 2221
[49] Millo O *et al* 2008 *Phys. Rev.* B **78** 092505
[50] Wang Y *et al* 2009 *Supercond. Sci. Technol.* **22** 015018
[51] Christianson A D *et al* 2008 *Nature* **456** 930
[52] Ding H *et al* 2008 arXiv:0812.0534
[53] Lu D H *et al* 2008 *Nature* **455** 18
[54] Chu C W *et al* 2008 *J. Phys. Soc. Japan* **77** 72
[55] Haule K, Shim J H and Kotliar G 2008 *Phys. Rev. Lett.* **100** 226402
[56] Shorikov A O *et al* 2008 arXiv:0804.3283
[57] Aryanpour K, Pickett W E and Scalettar R T 2006 *Phys. Rev.* B **74** 085117
[58] Merino J, Powell B J and McKenzie R H 2006 *Phys. Rev.* B **73** 235107
[59] Lu F, Wang W-H and Zou L-J 2008 *Phys. Rev.* B **77** 125117
[60] Manousakis E, Ren J and Kaxiras E 2008 *Phys. Rev.* B **78** 205112
[61] Dubroka A *et al* 2008 *Phys. Rev. Lett.* **101** 097011
[62] Ma F J, Lu Z-Y and Xiang T 2008 arXiv:0806.3526
[63] Kotliar G and Liu J L 1988 *Phys. Rev.* B **38** 5142
[64] Chubukov A V, Efremov D V and Eremin I 2008 *Phys. Rev.* B **78** 134512
[65] Mazina I I and Schmalianb J 2009 arXiv:0901.4790
[66] Yin Z P *et al* 2008 *Phys. Rev. Lett.* **101** 047001
[67] Zhao J *et al* 2008 *Phys. Rev. Lett.* **101** 167203